Materials Research Express

PAPER

Formation and analysis of the specific features of the electronic structure of an array of Ge/ZnSe nanoscale heterostructures

RECEIVED
28 September 2016

REVISED
10 October 2016

ACCEPTED FOR PUBLICATION
17 October 2016

PUBLISHED
3 November 2016

A N Beltiukov[1], F Z Gilmutdinov[1], R G Valeev[1], V V Mukhgalin[1], O V Boytsova[2,3] and V K Ivanov[3]

[1] Physical-Technical Institute of UB RAS, Izhevsk, Russia
[2] Lomonosov Moscow State University, Moscow, Russia
[3] Kurnakov Institute of General and Inorganic Chemistry of RAS, Moscow, Russia

E-mail: beltukov.a.n@gmail.com

Keywords: heterostructure, Ge, ZnSe, anodic alumina, valence band discontinuity, XPS

Abstract

This paper describes a method for forming an array of Ge/ZnSe nanoheterostructures by vacuum thermal evaporation. ZnSe and Ge layers were deposited on an anodic aluminum oxide surface with a pore diameter of 24 nm. Scanning electron microscopy showed that nanoheterostructures are formed in the pore channels. The features of the electron structure of the samples obtained were investigated by x-ray photoelectron spectroscopy and optic absorption spectroscopy. These investigations showed that the band gap of germanium increases. Also, there is a significant increase in valence band discontinuity (to 3.6 eV). Thus, we obtained Ge/ZnSe heterostructures with non-overlapping band gaps or broken-gap heterostructures.

1. Introduction

The technology of semiconductor heterojunctions holds an important place in modern electronics and optoelectronics. Its further development is focused on structures of the order of tens of nm and less than 10 nm, which have new properties different from those of higher-dimensional systems. Moreover, for some applications, in particular, for solar cells and LEDs, approaches are being developed to the formation of a textured surface of heterojunctions with micro- and nano- topography, which reduces optical losses but, on the other hand, may lead to an increase in the surface recombination rate due to an increased density of surface states [1, 2]. This motivates the interest in the study of the electronic structure of nanoscale heterostructures.

The heterojunction between Ge and ZnSe is now fairly well understood. For example, a series of papers [3–6] present both an experimental determination of band structure parameters and theoretical calculations of the Ge/ZnSe heterojunction, among other things, for the application as solar cells. Also, one-dimensional Ge/ZnSe heterojunctions with an atomically smooth boundary and axial nanowire heterostructures were obtained in [7, 8], but the band structure parameters were not defined. In [9], we proposed a method for forming nanostructured Ge/ZnS layers comprising an ordered array of core/shell nanostructures. This method is based on the thermal deposition of semiconductor layers onto the surface of porous alumina. In this paper we use this method to form nanoscale Ge/ZnSe heterostructures. In order to study the electronic structure features of the samples obtained, we have applied optical spectroscopy and x-ray photoelectron spectroscopy (XPS).

2. Experimental details

2.1. Sample preparation

The deposition of semiconductor layers was carried out in a high-vacuum thermal evaporation chamber. The vacuum system had no oil sealed vacuum pumps. A magnetic-discharge pump was used to generate high vacuum (10^{-6} Pa). Two resistive evaporators were installed in the chamber to evaporate ZnSe and Ge, which made it possible to obtain heterojunctions in one working cycle. Anodic alumina matrices were used as a substrate.

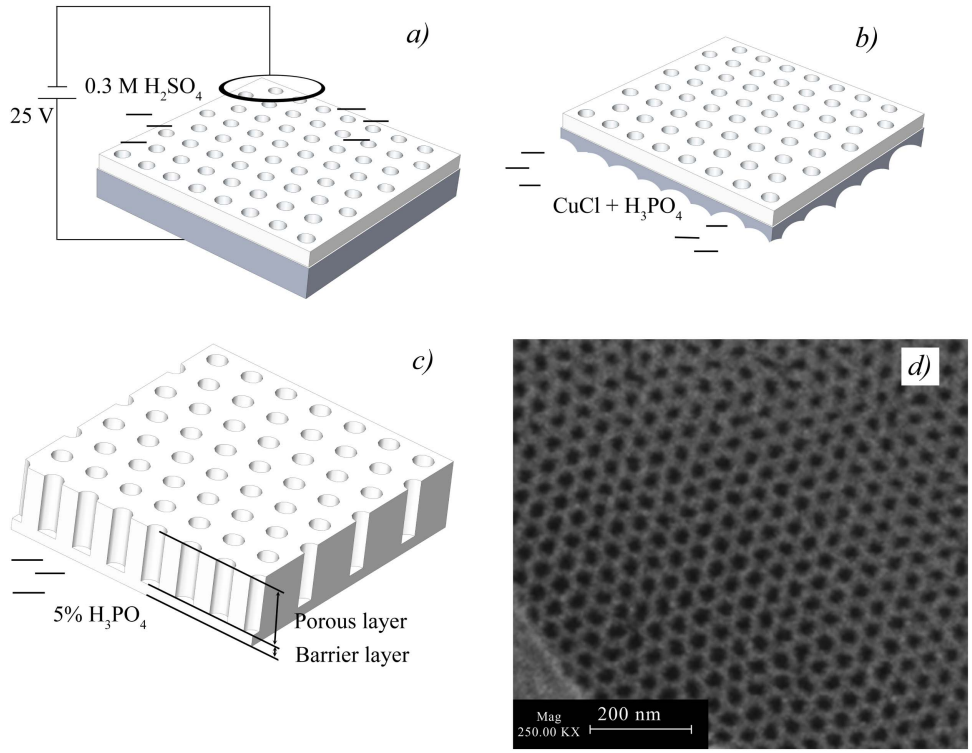

Figure 1. Preparation of the AAO matrix: (a) Al anodization in 0.3 M H_2SO_4, (b) removal of aluminum residues in $CuCl + H_3PO_4$, (c) removal of the barrier layer in 5% H_3PO_4, (d) SEM image of AAO.

Anodic aluminum oxide (AAO) has a unique porous structure with ordered or quasi-ordered arrangement of cylindrical pores. The porosity parameters (pore diameter and distance between the centers of adjacent pores) depend on the electrolyte used for anodization and on the applied voltage [10]. AAO matrices were prepared by the anodic oxidation of a preannealed and mirror polished aluminum plate (99.999%) in a 0.3 molar solution of the sulfuric acid H_2SO_4 at 0 °C and 25 V voltage. After anodization, the aluminum residues were removed in a copper chloride solution with phosphoric acid. The thin nonporous alumina layer (barrier layer) formed during anodization and separating the metal substrate and the porous layer was removed in 5% H_3PO_4 solution. After removal of the barrier layer, the surface on the side where the barrier layer was has a more ordered arrangement of pores, therefore the semiconductor layers were deposited on this side (figure 1). The morphology of the sample surfaces was investigated by a scanning electron microscope (SEM) Carl Zeiss NVision 40-38-50. The pore diameter was 24 $\pm$ 1 nm, and the distance between pores was 60 $\pm$ 2 nm.

The formation of the heterojunction was started by depositing a ZnSe layer, which led to a decrease in the pore diameter to 20 $\pm$ 2 nm. Then the Ge layer was deposited. As a result, the pores closed almost completely (figure 2). The substrate temperature during the deposition did not exceed 300 °C. The material covered the AAO surface uniformly, gradually filling the pores and forming nanostructures in their channels. In what follows the samples obtained are denoted as Ge/ZnSe/AAO. Under the same conditions, a comparison sample was prepared, in which fused silica was used as the substrate. This comparison sample is denoted as Ge/ZnSe/SiO_2.

2.2. Research methods

To analyze the morphology of the nanostructures formed in the pore channels by scanning electron microscopy, we fixed the samples on a metal substrate with a carbon tape. Then alumina was removed in a chromic solution at 80 °C. The remaining investigations were conducted on the samples with the AAO matrix on the side of the ZnSe and Ge semiconductor layers.

The crystal structure of the samples was analyzed on the D8 Advance x-ray diffractometer (Bruker AXS) with Cu Kα radiation. Registration was carried out in the grazing incidence mode at a fixed incident angle of 0.2°. The accumulation time at the point was 10 s. Under these conditions, the depth of the analyzed layer was about 280 nm. The phase analysis was performed using the JCPDS structural database.

The XPS sample was investigated using a laboratory spectrometer made by SPECS. The spectra were recorded using MgKα excitation. The processing of the experimental data was done using CasaXPS software.

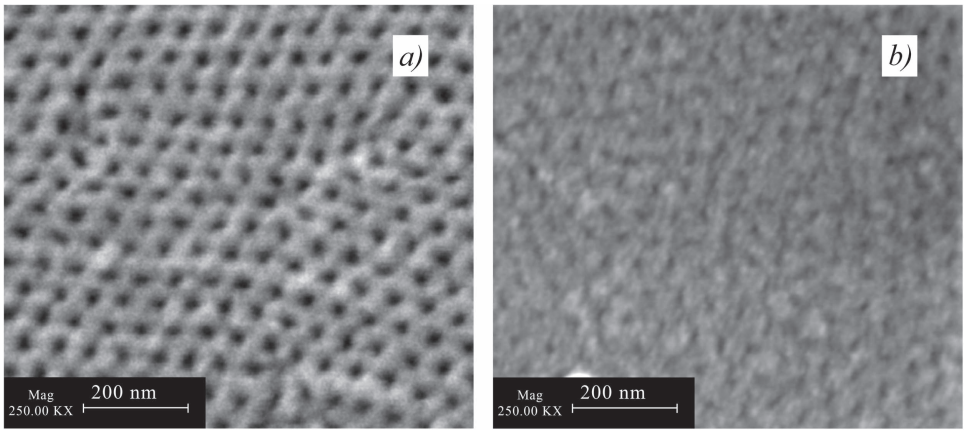

Figure 2. SEM images after depositing first a ZnSe layer 30 nm in thickness (a) and then a Ge layer 60 nm in thickness (b).

The determination and subtraction of the background line was performed according to the Shirley algorithm [11]. To determine the positions of germanium core levels on the uncleaned sample, we used a C 1s carbon line with natural hydrocarbon contaminations as a reference. The carbon binding energy was 285 eV.

The optical properties of the samples were investigated by UV/Vis spectroscopy. Transmission and reflection spectra were obtained on the Lambda 950 spectrometer (PerkinElmer) and converted to optical density by the formula

$$D = \ln\{(1 - R)^2/T\},$$

where R and T are the reflection and transmission coefficients, respectively. To determine the bandgap of semiconductor layers, the self-absorption edge was plotted in accordance with the Tauc law [12]

$$(Dhv)^{1/2} = B^{1/2}(hv - E_g),$$

where hv is the photon energy, B is the Tauc constant proportional to the density of electronic states (DOS), E_g is the optical bandgap defined by linear extrapolation at the intersection with the abscissa axis.

3. Results and discussion

3.1. Investigations of the morphology and crystal structure of Ge/ZnSe/AAO

Figure 3 presents a SEM image of the film remaining after removal of the AAO matrix. The surface of the film is uniformly covered with nanostructures in the form of tubes or rings, the arrangement of which repeats the arrangement of the pores of the original matrix. However, the diameter of the nanorings (30 $\pm$ 3 nm) is slightly larger than that of the pores of the original matrix (24 $\pm$ 1 nm).

The inner diameter of the nanorings is 12 nm. The pattern of pore overgrowing during deposition indicates that the outer shell of the nanoring consists of a 2 nm ZnSe layer and the inner shell consists of a Ge layer. Note that the thickness of the Ge layer in the nanostructure located in the matrix pore should be of the order of 4 nm. The samples obtained can be described as nanostructured layers containing arrays of nanoscale axial Ge/ZnSe heterostructures.

Figure 4 presents XRD pattern of the Ge/ZnSe/AAO sample and bar representations of Ge and ZnSe sphalerite phase. A broad amorphous halo from the porous alumina is observed at the base of the first peak. The small difference of the parameters of the germanium crystal lattice (5.66 Å, JCPDS 81-683) and the sphalerite phase of zinc selenide (5.67 Å, JCPDS 5-552) leads to the merging of reflections from their planes. It makes impossible to determine the contributions of Ge and ZnSe to the diffraction peaks. Calculations showed the average value of the lattice constant of the samples is 5.63 $\pm$ 0.01 Å. This value is smaller than the lattice constant of bulk germanium and bulk zinc selenide. The lattice distortions indicate compressive stresses arising in the nanostructures during formation in a closed volume. Thus, the increase in the nanorings' diameter after removal of the oxide matrix is possible due to the relaxation of mechanical stresses.

3.2. XPS investigations

The chemical composition of the samples obtained was investigated by XPS with an accuracy characteristic of this method. On the obtained spectra there are lines of germanium, zinc and selenium (figure 5). Since the photoelectron escape depth is not more than a few nanometers, photoelectrons from the Ge and ZnSe layers as

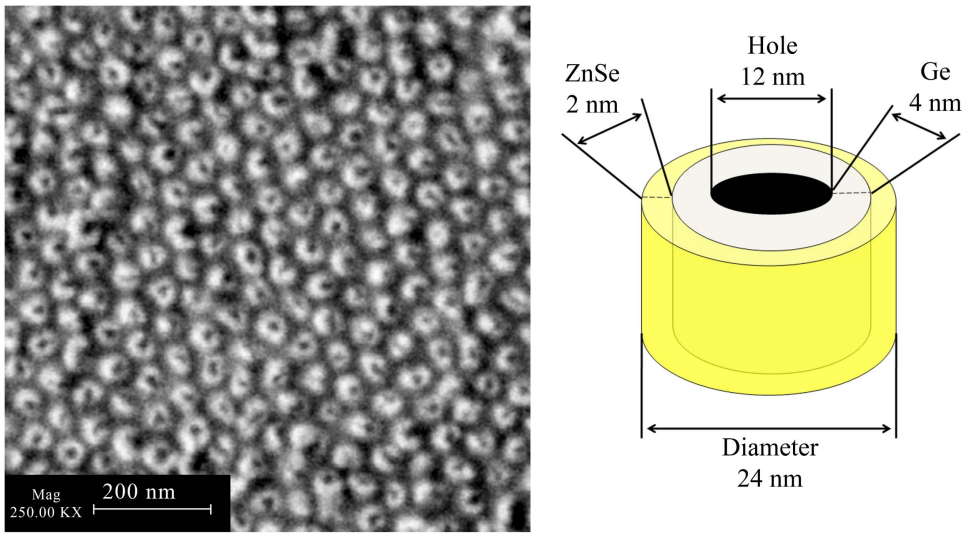

Figure 3. Ge/ZnSe nanoscale heterostructures after removal of the AAO matrix and the schematic image of the Ge/ZnSe nanoheterostructure.

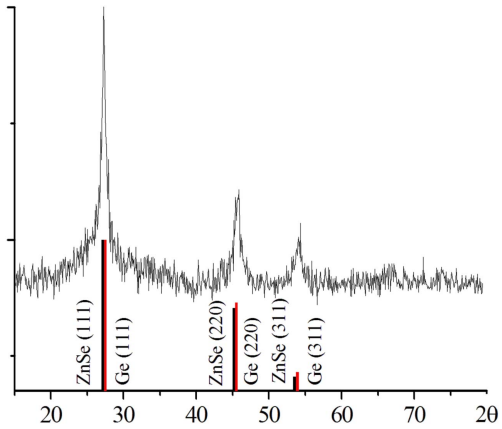

Figure 4. XRD pattern of Ge/ZnSe/AAO.

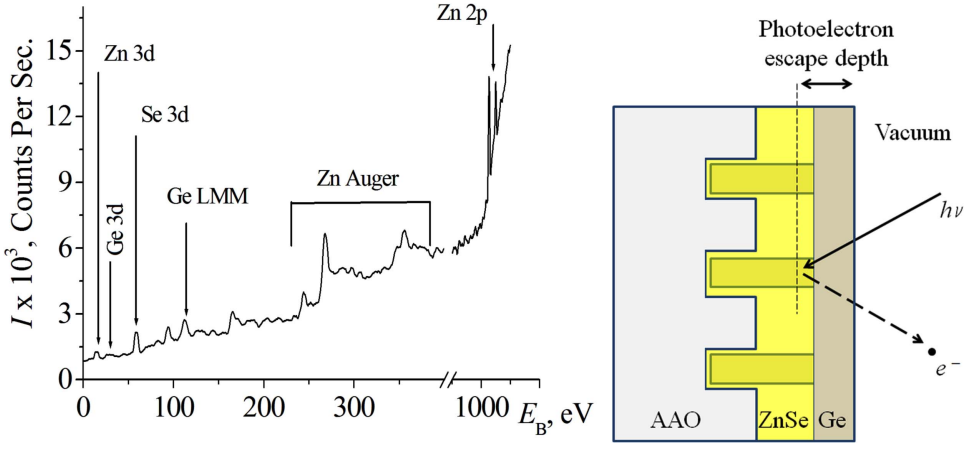

Figure 5. XPS spectra and schematic diagram of the photoemission region of the Ge/ZnSe/AAO sample.

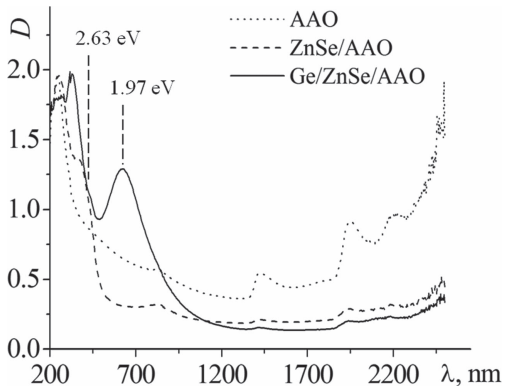

Figure 6. The optical density spectra of the AAO matrix (dotted line), the deposited layer of ZnSe on AAO (dashed line) and the deposited layers of Ge and ZnSe on AAO (solid line).

well as from the area of Ge/ZnSe nanoheterostructures contribute to the spectrum. In fact, the resulting spectrum can be represented as a superposition of individual germanium and zinc selenide spectra shifted relative to each other due to an offset of the energy bands at the heterojunction interface. This shift allows one to determine the valence band discontinuity of the heterojunction. The change in the distance between the core levels of two semiconductors $\delta(\Delta E_B)$ separated by the heterojunction interface is equal to the change in the value of the valence band discontinuity $\delta(\Delta E_V)$ [13]. In this case the valence band discontinuity can be expressed as follows:

$$\Delta E_V = [E_{Ge3d}\,(Ge) - E_{Zn3d}\,(ZnSe)]_{Bulk} - [E_{Ge3d}\,(Ge) - E_{Zn3d}\,(ZnSe)]_{HJ},$$

where $[E_{Ge3d}\,(Ge) - E_{Zn3d}\,(ZnSe)]_{Bulk}$ is the binding energy difference between the core levels for the bulk semiconductors and $[E_{Ge3d}\,(Ge) - E_{Zn3d}\,(ZnSe)]_{HJ}$ is that for the heterojunction under study. In our case, the valence band discontinuity calculated by this formula was 3.6 ± 0.2 eV for the Ge/ZnSe/AAO sample. The calculated value is much higher than ΔE_V for the two-dimensional Ge/ZnSe heterojunction on a single crystal substrate (1.4 eV [3, 4]). For the comparison sample Ge/ZnSe/SiO_2 ΔE_V is 1.2 ± 0.2 eV. The energy band offset is influenced by many factors, the most important of which are the crystal plane orientation of semiconductor layers, interdiffusion, and the presence of extraneous layers on the interface [14]. No impurities have been detected in the heterostructures obtained by XPS. The interdiffusion effect at a relatively low deposition temperature (300 °C) should be minimal. Therefore, the significant increase in ΔE_V is mainly determined by the influence of the orientation of Ge and ZnSe crystal planes. In addition, the crystal lattice distortion also has a significant impact. The study of the valence band discontinuity in the strained Ge–Si heterosystems has shown that as the lattice constant decreases, ΔE_V increases [15]. Thus, based on the XRD data, we can conclude that ΔE_V increases to 3.6 eV due to the distortion of the germanium crystal lattice.

3.3. Optical absorption spectroscopy

The optical density spectra of the initial AAO matrix and the matrix with the ZnSe and Ge/ZnSe layers deposited are presented in figure 6. Since the semiconductor layers are much thinner than the matrix, porous alumina makes the main contribution to the optical spectra. The features of the AAO absorption in the short-wave region of the spectrum are due to the oxygen defects [16]. The ZnSe deposition gives rise to an absorption band with an edge at 2.63 ± 0.05 eV, which determines the band gap of the semiconductor. After Ge deposition, another absorption band appears. The maximum of this band is near 2 eV, which can be linked to the direct band transition in Ge, but is shifted to the short wavelength region [17].

To investigate the absorption edge of the sample in more detail, we have used the Tauc law [14]. Figure 7 shows Tauc plots, $(Dh\nu)^{1/2}$ versus $h\nu$, of Ge/ZnSe/AAO and Ge/ZnSe/SiO_2 sample spectra (thin films on a silica substrate). As can be seen, on the Ge/ZnSe/AAO spectrum there is no fundamental absorption edge of germanium at 0.67 eV, and it is blue shifted relative to the spectrum of Ge/ZnSe/SiO_2. The optical band gap of Ge nanostructures equals nearly 1.39 eV. The blue shift can be due to changes in the electronic structure caused by mechanical stresses in Ge/ZnSe/AAO nanoheterostructures. On the other hand, since the nanostructures in the alumina pore channels contain germanium layers of 4 nm, the appearing quantum confinement effect can also cause an extension of the band gap [18, 19]. Unfortunately, we have not been able to determine which of these two effects takes place. This requires further investigations.

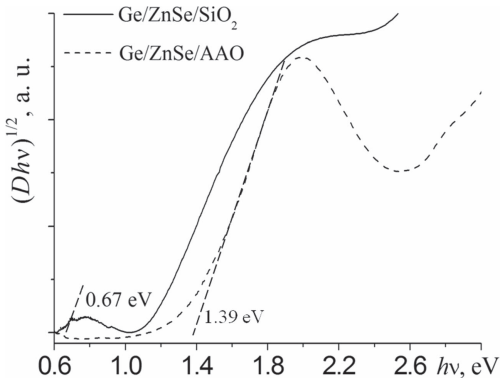

Figure 7. The absorption edge of the Ge/ZnSe heterostructure on silica (solid line) and AAO (dashed line).

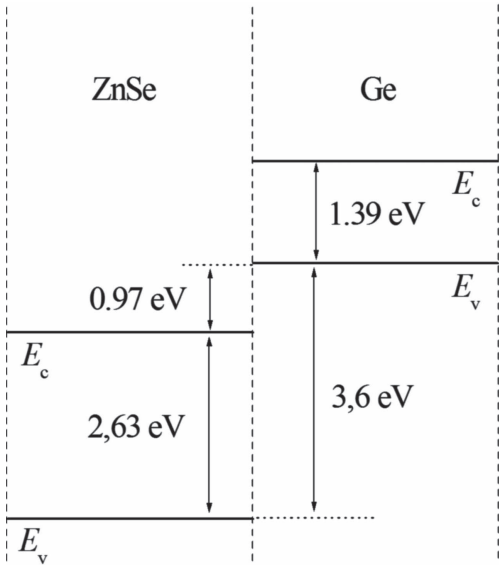

Figure 8. Schematic band structure of Ge/ZnSe/AAO.

3.4. Schematic band structure of Ge/ZnSe/AAO

In figure 8 we present a schematic band structure of Ge/ZnSe/AAO without considering band bending. The bottom of the ZnSe conduction band lies approximately 0.97 eV below the top of the Ge valence band, leading to a broken gap heterojunction. The type of broken-gap heterojunctions that is now particularly well understood is the GaSb/InAs superlattice. The electrons decreasing their energy flow from the overlying valence band of one semiconductor to the underlying conduction band of another semiconductor [20]. They build an electronic channel whose properties can be modulated by light, electric or magnetic fields [21]. Thus, the interface nanostructuring of the Ge/ZnSe heterostructure system can lead to significant changes in its electronic structure and to new properties. The formation of nanoscale heterojunctions and their introduction into the structure of the semiconductor device may be one of the areas of 'band engineering'.

4. Conclusion

In this paper, an array of axial heterostructures in the form of nanorings has been obtained by vacuum thermal deposition of Ge and ZnSe semiconductors on the surface of porous alumina. The study of the electronic structure of the samples showed a significant difference from the two-dimensional heterojunctions of Ge/ZnSe on the single crystal substrates. The lattice distortions arising during the formation of nanostructures in a closed volume of alumina pores lead to an increase in the valence band discontinuity to 3.6 eV. Also, the germanium bandgap increases significantly, which may be associated with the quantum confinement effect or mechanical

stress of the crystal lattice. Thus, the surface nanostructuring may be one way to control the electronic properties of heterojunctions and provides new opportunities for the development of semiconductor devices.

Acknowledgments

The authors are grateful to researchers of the Collaborative Access Centers of the Physical Technical Institute of UB RAS, Kurnakov Institute of General and Inorganic Chemistry of RAS and the Lomonosov Moscow State University for the opportunity to carry out investigations using their equipment. This work was supported by the Russian Foundation for Basic Research (project No 14-32-50276).

References

[1] Dmitruk N L *et al* 2015 *Solar Energy Mater. Solar Cells* **137** 124–30
[2] Gan J, Ramakrishnan S and Yeoh F Y 2015 *Rev. Adv. Mater. Sci.* **42** 92–101
[3] Margaritondo G 1984 *Solid State Commun.* **52** 495–8
[4] Duran J C, Munoz A and Flores F 1987 *Phys. Rev.* B **35** 7721–4
[5] Da-Yan B *et al* 1996 *Acta Phys. Sin.* **5** 590–600
[6] Sahai R and Milnes A G 1970 *Solid-State Electron.* **13** 1289–99
[7] Xu X *et al* 2011 *Chem. Phys. Lett.* **501** 491–5
[8] Kang K *et al* 2014 *Nanotechnology* **25** 014010
[9] Beltiukov A *et al* 2014 *Phys. Status Solidi* c **11** 1452–4
[10] Poinern G E J, Ali N and Fawcett D 2011 *Materials* **4** 487–526
[11] Shirley D A 1972 *Phys. Rev.* B **5** 4709–13
[12] Cosentino S *et al* 2011 *Nanoscale Res. Lett.* **6** 135
[13] Grant R W, Waldrop J R and Kraut E A 1978 *Phys. Rev. Lett.* **40** 656
[14] Bauer R S and Sang H W Jr 1983 *Surf. Sci.* **132** 479–504
[15] Ke S, Wang R and Huang M 1995 *Solid State Commun.* **93** 1009–12
[16] Mukhurov N I *et al* 2010 *J. Appl. Spectrosc.* **77** 549–55
[17] Philipp H P and Taft E A 1959 Optical constants of germanium in the region 1 to 10 eV *Phys. Rev.* **113** 1002–4
[18] Shan B and Cho K 2005 *Phys. Rev. Lett.* **94** 236602
[19] Takagahara T and Takeda K 1992 *Phys. Rev.* B **46** 15578–81
[20] Sai-Halasz G A, Esaki L and Harrison W A 1978 *Phys. Rev.* B **18** 2812
[21] Voronina T I *et al* 2001 *Semiconductors* **35** 331–7